

Observational evidence for solar wind proton heating by ion-scale turbulence

G. Q. Zhao^{1,2}, Y. Lin³, X. Y. Wang³, D. J. Wu⁴, H. Q. Feng¹, Q. Liu¹, A. Zhao¹, and H. B. Li¹

¹Institute of Space Physics, Luoyang Normal University, Luoyang, China

²Henan Key Laboratory of Electromagnetic Transformation and Detection, Luoyang, China

³Physics Department, Auburn University, Auburn, USA

⁴Purple Mountain Observatory, CAS, Nanjing, China

Key Points:

- Nearly collisionless solar wind turbulence at ion scales is investigated with 11 years of in-situ data
- Correlations between the spectral index and magnetic helicity, and between the proton temperature and turbulent energy are revealed
- A scenario for the solar wind turbulence and heating at ion scales is proposed

arXiv:2009.00120v1 [physics.space-ph] 31 Aug 2020

Abstract

Based on in-situ measurements by Wind spacecraft from 2005 to 2015, this letter reports for the first time a clearly scale-dependent connection between proton temperatures and the turbulence in the solar wind. A statistical analysis of proton-scale turbulence shows that increasing helicity magnitudes correspond to steeper magnetic energy spectra. In particular, there exists a positive power-law correlation (with a slope ~ 0.4) between the proton perpendicular temperature and the turbulent magnetic energy at scales $0.3 \lesssim k\rho_p \lesssim 1$, with k being the wavenumber and ρ_p being the proton gyroradius. These findings present evidence of solar wind heating by the proton-scale turbulence. They also provide insight and observational constraint on the physics of turbulent dissipation in the solar wind.

Plain Language Summary

The solar wind is a tenuous magnetized plasma that serves as a natural laboratory of nearly collisionless turbulence. It is streaming outward from the Sun and has temperatures much higher than those from a spherically expanding ideal gas, implying a heating process must occur. The heating has been extensively discussed in past decades, but still not well understood. Based on in-situ measurements, we reveal a scale-dependent connection between proton temperatures and the turbulence with enhanced magnetic helicity signature. The connection is particularly strong for the proton temperature in the direction perpendicular to the background magnetic field. These observations provide implications for the physics of turbulent dissipation and heating in a collisionless plasma.

1 Introduction

It is well known that the solar wind is pervaded with magnetic fluctuations that are inherently turbulent. The fluctuation energy appears as a power-law spectrum over a broad range of spacial scales (Alexandrova et al., 2013; Bruno & Carbone, 2013). The energy-containing range indicates very large scales with frequencies $f < 10^{-4}$ Hz in the spacecraft reference frame. The energy spectrum in this range goes as $\sim f^{-1}$, and is interpreted as uncorrelated large-scale Alfvén waves that provide a source of energy. The inertial range represents intermediate scales with spacecraft frame frequencies $10^{-4} \lesssim f \lesssim 10^{-1}$ Hz. The spectrum follows a $f^{-5/3}$ law that is dominated by the Kolmogorov cascade. At small scales comparable to the proton gyroradius or inertial length, the spectrum becomes complicated with various spectral indices between -2 and -4 (e.g., Sahraoui et al., 2013; Bruno et al., 2014), frequently lower than the classic index $-7/3$ predicted by strong-turbulence theory for dispersive cascade (Galtier, 2006; Wu & Chen, 2020). The spectral steepening at the small scales are often interpreted as the occurrence of turbulent dissipation due to cyclotron damping (Gary & Borovsky, 2004; Smith et al., 2012), Landau damping (He, Pei, et al., 2015; Howes et al., 2018), stochastic heating (Johnson & Cheng, 2001; Chandran et al., 2010), or plasma coherent structures such as current sheets and magnetic vortices (Perri et al., 2012; Wang et al., 2019).

Various studies were conducted to explore the nature of the proton-scale turbulence in the solar wind, which is fundamentally important to the understanding of the dissipation and heating. Two models were proposed theoretically, including kinetic Alfvén wave (KAW) and whistler wave turbulence models (Gary & Smith, 2009). KAW turbulence model was suggested by a large body of studies on the basis of observations (e.g., Bale et al., 2005; Sahraoui et al., 2009; Howes & Quataert, 2010; He et al., 2012a; Podesta, 2013) and simulations (Howes et al., 2008; Grošelj et al., 2018). Among them, several studies used non-zero magnetic helicity to diagnose the presence of KAWs in the turbulence (Howes & Quataert, 2010; He et al., 2012a; Podesta, 2013). The KAW turbulence would heat the solar wind through cyclotron/Landau damping or stochastic heating, while

it is under debate which process is dominant (Parashar et al., 2015; Isenberg & Vasquez, 2019).

The issue on the heating of the solar wind is complicated because of the complex roles of double-adiabatic expansion, global heat flux, ion differential flows, Coulomb collisions, local wave action, microinstabilities, and turbulence (see a recent review by Verscharen et al., 2019). Various correlations in the solar wind have been reported. Proton temperatures are found to be correlated with the solar wind speed, and faster solar wind usually corresponds to higher proton temperatures (Marsch et al., 1982; Newbury et al., 1998). Steeper spectra at proton scales are also linked to faster solar wind (Bruno et al., 2014). The faster solar wind tends to be more imbalanced with greater wave energy flux anti-sunward than sunward (Tu & Marsch, 1995). These correlations with the solar wind speed are possibly a consequence of different source populations of the solar wind (Schwenn, 2006). There is also a correlation between the temperature ratio of alpha particles to protons and the alpha–proton differential flow (Kasper et al., 2008). This has been interpreted as evidence of solar wind heating by field-aligned ion-cyclotron waves (Gary et al., 2006; Kasper et al., 2013). A link between inertial-range intermittency and proton temperature enhancement has also been reported, as evidence of nonuniform heating driven by magnetohydrodynamic turbulence (Osman et al., 2011, 2012).

In this letter, we report a new correlation between the spectral steepness and magnetic helicity for nearly collisionless solar wind turbulence at proton scales. The correlation exists even within a very narrow range of the solar wind speed. Moreover, it is shown that the proton perpendicular temperature is correlated with the turbulent magnetic energy at proton scales. A higher magnetic helicity favors a better correlation of the temperature with the magnetic energy. These findings will provide improved understanding of the ion-scale turbulence and heating in the solar wind.

2 Data and Analysis Methods

The data used in this letter are from the Wind spacecraft. The magnetic field data are from the Magnetic Field Investigation instrument and have a cadence of 0.092 s, (Lepping et al., 1995). The plasma data are from the Solar Wind Experiment instrument working at a cadence of 92 s (Ogilvie et al., 1995). The proton temperatures are produced via a nonlinear-least-squares bi-Maxwellian fit of ion spectrum from the Faraday cup (Kasper et al., 2006). The data set is surveyed from 2005 to 2015 through dividing the long time series into consecutive and overlapping time segments. In each segment with data available, the magnetic energy spectrum is obtained via standard fast Fourier transform technique. The plasma parameters, including the proton density N_p , perpendicular and parallel thermal velocities $w_{\perp p}$ and $w_{\parallel p}$, and bulk velocity \mathbf{V}_p , are given as average values over the time segment, where \perp and \parallel are with respect to the ambient field \mathbf{B}_0 . Each time segment has a span of 200 s, a compromise time interval to reduce the averaging effects for plasma parameters while to cover the magnetic spectrum of interest with an appropriate resolution simultaneously. An overlap is set to be 100 s, comparable to the plasma data cadence. The Coulomb collisional age A_c is calculated, which is the ratio of the transit time of the solar wind to the collision timescale (Livi et al., 1986). Segments with $A_c < 0.1$ are selected for samples with negligible collision effects. This selection means that the faster solar wind would be chosen in principle. The selected segments have a median of the solar wind speed being 519 km s^{-1} , while it is 388 km s^{-1} for all segments. It is also required that the angle between \mathbf{B}_0 and \mathbf{V}_p is in the range from 60° to 120° to reduce possible heating/cooling effects due to the alpha–proton differential flow, which could be strong when \mathbf{B}_0 and \mathbf{V}_p are quasi-parallel (Zhao et al., 2020; Zhao, Li, et al., 2019). In total about 2.6×10^5 time segments satisfying these constraints are selected, and most (95%) of them have proton parallel beta in the range from 0.1 to 3.

The normalized reduced magnetic helicity is considered as an indicator of the presence of polarized waves in this letter. The helicity is a measure of the spatial handedness of the magnetic field, and has been widely used to identify wave modes in the solar wind for nearly parallel propagating cyclotron waves (Zhao et al., 2018; Zhao, Feng, et al., 2019; Woodham et al., 2019) or oblique KAWs (Howes & Quataert, 2010; He et al., 2011). The helicity refers to the fluctuating helicity in spectral form and is defined as $H_m(\mathbf{k}) \equiv \mathbf{A}(\mathbf{k}) \cdot \mathbf{B}^*(\mathbf{k})$, where \mathbf{A} is the fluctuating magnetic vector potential, \mathbf{B} is the fluctuating magnetic field, the asterisk represents the complex conjugate of the Fourier coefficients, and \mathbf{k} is the wave vector (Matthaeus & Goldstein, 1982; Woodham et al., 2019). For the magnetic field measured by a single spacecraft, only the reduced helicity spectrum is available, which can be written as $H_m^r(k_1) = 2\text{Im}[B_2(k_1) \cdot B_3^*(k_1)]/k_1$ (Matthaeus & Goldstein, 1982; Woodham et al., 2019), where k_1 is the reduced wavenumber and the direction 1 is the direction in which the spectrum is reduced, Im means the imaginary part, and $B_2(k_1) \cdot B_3^*(k_1)$ is an element in the energy spectral tensor. The normalized reduced magnetic helicity is defined as $\sigma_{k_1} = k_1 H_m^r(k_1)/P_{k_1}$, which takes values between $[-1, 1]$, where $P_{k_1} = |\mathbf{B}(k_1)|^2$ is the total magnetic energy at wavenumber k_1 . In practice we first calculate the magnetic helicity as a function of frequency instead of wavenumber, i.e., $\sigma_f = 2\text{Im}[B_y(f) \cdot B_z^*(f)]/P_f$, where f is the frequency associated with the spacecraft time series of measured magnetic field in the GSE coordinate system. The calculation of σ_f is allowed when Taylor frozen-in-flow hypothesis holds, by which the frequency is related to wavenumber (Taylor, 1938; Matthaeus & Goldstein, 1982; He et al., 2011).

A statistical examination is conducted for the nature of the solar wind turbulence. The examination is according to the direction of the long axis of magnetic fluctuations with respect to local \mathbf{B}_0 . It is expected that the long axis is quasi-perpendicular to \mathbf{B}_0 for KAW turbulence but to be quasi-parallel for whistler wave turbulence based on the linear kinetic theory (He et al., 2012a). To determine the long axis of the fluctuations, variance analysis technique is adopted to estimate the long-axis direction, which has maximum variance of fluctuations (Sonnerup & Scheible, 1998). A large θ_{LB} , the angle between the long axis and local \mathbf{B}_0 , could be expected if it is KAW turbulence.

Figure 1 presents an example to illustrate the parameters used in this letter. Figure 1a plots the magnetic energy spectrum (P_f) in the frequency domain (for data on 5 June 2005, 01:33:23–01:36:43 UT). The spectrum follows the $f^{-5/3}$ law in the low frequency, and steepens with an index about -2.8 when the frequency exceeds 0.4 Hz. With the frequency approaching 2 Hz, the spectrum flattens again possibly due to the instrument noise and/or aliasing. The two vertical dashed lines in Figure 1a indicate the range of interest in this letter. The left line corresponds to a wavenumber $k\rho_p = 0.1$, where $\rho_p = w_{\perp p}/\Omega_p$ is the proton thermal gyroradius and Ω_p is the proton cyclotron frequency. The right line is chosen accordingly with $P_f > 10^{-3}$ nT²/Hz that is required for signal level much higher than the instrument noise level (Lepping et al., 1995). The wavenumber k represents the reduced wavenumber and is calculated by the Taylor frozen-in-flow hypothesis (Taylor, 1938), $2\pi f = kV_p$, with which the frequency domain can be converted to the wavenumber domain. Figure 1a is then replotted as Figure 1b, with P_k instead of P_f for the range bounded by the vertical dashed lines in Figure 1a. In this step an averaging operation is performed to show a smoothed spectrum; the running average window runs over $fe^{-0.5} \leq f \leq fe^{0.5}$. A similar averaging is performed for magnetic helicity spectrum, and the smoothed σ_k is shown in Figure 1c. The helicity σ_k is obviously non-zero at $k\rho_p \sim 1$ in this example. The drop of σ_k at $k\rho_p > 1$ could be attributed to the noise and/or aliasing (Klein et al., 2014). It also could be attributed to the greater balance of KAW turbulence or nonlinear effects at smaller scales that will weaken the helicity signature (He et al., 2012b; Markovskii & Vasquez, 2013).

Figure 1d displays the local spectral index α_k , which is determined by the energy spectrum over the same frequency range for the averaging. The index α_k is around $-5/3$

within uncertainty when $k\rho_p < 0.25$; the large uncertainty is inherently due to the short time segment of 200 s that leads to an inefficient coverage for the inertial range. For $k\rho_p > 0.25$, the index α_k rapidly decreases to a more negative value, ~ -2.8 at $0.6 < k\rho_p < 1.5$. Note that the more negative α_k occurs with helicity signature enhanced as shown in Figure 1c. The presence of the more negative α_k with the higher helicity allows one to speculate that the steep energy spectrum might be partly attributed to the dissipation of the turbulence with enhanced helicity. An examination on the long-axis direction of magnetic fluctuations, Figure 1e, gives $\theta_{LB} > 80^\circ$ for $0.6 < k\rho_p < 1.5$, which is in line with the model of KAW turbulence (He et al., 2012a).

3 Statistical Results

Statistical investigations are performed to explore the significance of the results in Figure 1. It is found that spectral indices are ordered by the magnetic helicity at proton scales. As an example for $k\rho_p = 0.8$, Figure 2 displays, from top to bottom, distribution of $|\sigma_k|$, medians of α_k and θ_{LB} sorted by $|\sigma_k|$, where $|\sigma_k|$ is the absolute value of σ_k that can be either positive or negative even for a specific wave mode, depending on the directions of \mathbf{B}_0 and wave propagation with respect to the Sun. The distribution of $|\sigma_k|$ has a weak peak at $|\sigma_k| \sim 0.22$, and about 61% of the data have $|\sigma_k| > 0.15$. As $|\sigma_k|$ increases from 0 to 0.4, it is clear that the median of α_k decreases from about -2.2 to -3.2 (Figure 2b), implying a significant correlation between α_k and $|\sigma_k|$. From Figure 2c, statistical examination concerning the nature of the related turbulence shows that 91% (63%) of the data have $\theta_{LB} > 60^\circ$ (80°), and there is a tendency of θ_{LB} increasing with $|\sigma_k|$. If we consider only those data with maximum variances of magnetic fluctuations at least 10 times larger than other variances from orthogonal directions in the examination, the corresponding percentage increases to 98% (83%). Such large percentage supports KAW turbulence dominating the nearly collisionless solar wind at proton scales (He et al., 2012a).

One may speculate that the correlation between α_k and $|\sigma_k|$ is possibly a consequence of the scaling with solar wind speed V_p . Figure 2d is presented for this issue. In Figure 2d, different curves are for different sub-datasets bounded by V_p , where the red, orange, green, blue, light blue curves correspond to the V_p ranges of 400–450, 450–500, 500–550, 550–600, > 600 km s⁻¹, respectively. One can see that the correlation exists for each sub-dataset even when the V_p range is narrow (50 km s⁻¹). This should imply that the correlation of α_k with $|\sigma_k|$ is common and does not result from the scaling with the solar wind speed.

Another important finding in this letter is that proton temperature T_p is correlated with turbulent energy P_k . The correlation is particularly strong for $T_{\perp p}$ and depends on k , $|\sigma_k|$, and $\beta_{\parallel p}$, where T_p and $T_{\perp p}$ are the total and perpendicular temperatures of protons, respectively, $\beta_{\parallel p} = w_{\parallel p}^2/v_A^2$ is the proton parallel beta, v_A is the Alfvén speed. Higher $|\sigma_k|$ contributes to a better correlation according to our tests. Figure 3 plots the distributions of $(P_k, T_{\perp p})$ at fixed scales of (a) $k\rho_p = 0.5$ as well as (b) $k\rho_p = 0.8$. All data in the figure are bounded by $|\sigma_k| > 0.15$ and by $0.8 \leq \beta_{\parallel p} \leq 1$, producing the data with a size $N \simeq 2.3 \times 10^4$. The black dashed lines present linear fitting of the data in logarithmic space, describing a positive power law for the correlation between $T_{\perp p}$ and P_k at the proton scales. The slopes of the fitting lines are considerable, 0.38 at $k\rho_i = 0.5$ and 0.39 at $k\rho_i = 0.8$. The relative uncertainties are found to be very small, $\sim 1\%$.

Again, one may keep in mind that the solar wind speed could play a role in the correlation shown in Figure 3. To make this issue clear, Figures 3c and 3d plot the distributions of (P_k, V_p) at fixed scales of $k\rho_p = 0.5$ and $k\rho_p = 0.8$, respectively. The distributions are shown to be significantly dispersive, although there is a tend of positive correlation between V_p and P_k . Following the plot of Figures 3a and 3b, five sub-datasets with different V_p ranges, as displayed in Figure 2d, are checked. Results show that the

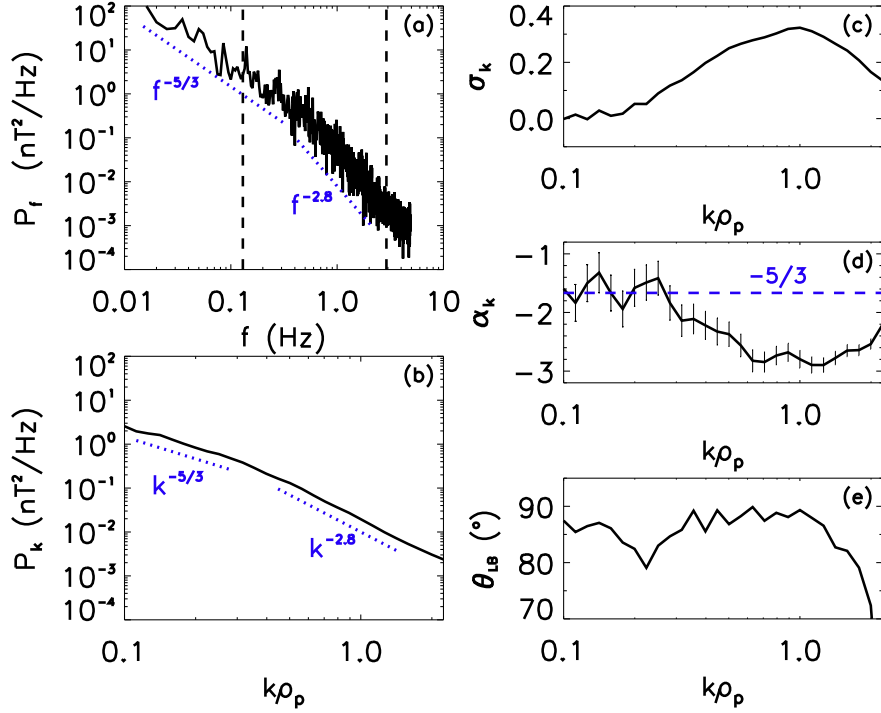


Figure 1. An example for a time segment of 200 s on 5 June 2005 to illustrate parameters used in this letter: (a) magnetic energy P_f ; (b) local average magnetic energy P_k ; (c) local average magnetic helicity σ_k ; (d) local spectral index of magnetic energy α_k ; (e) the angle between the long axis of magnetic fluctuations and \mathbf{B}_0 , θ_{LB} . Two vertical dashed lines in (a) indicate the range shown in (b)–(e) in wavenumber domain.

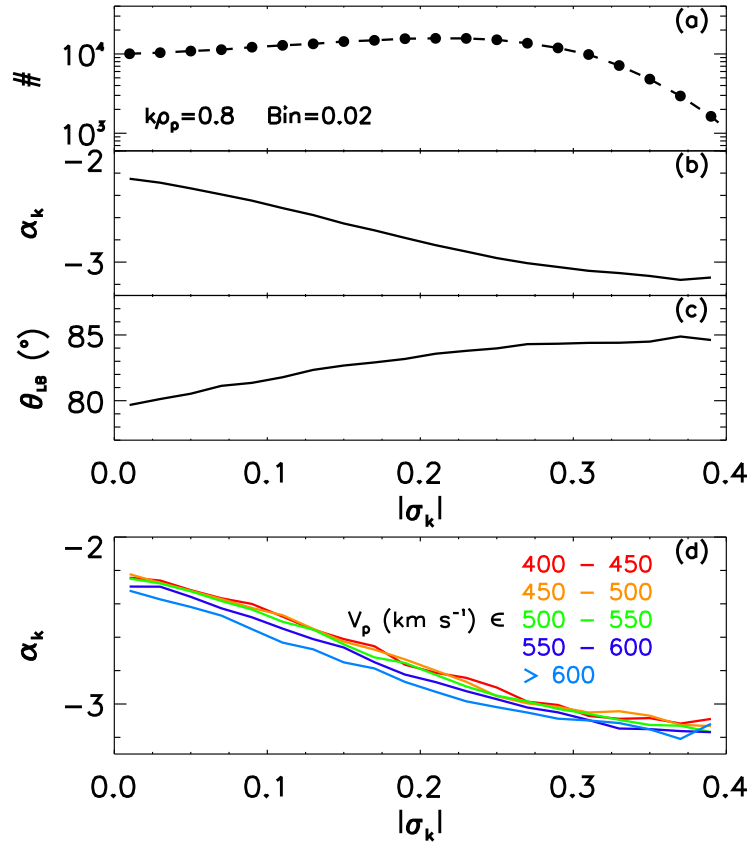


Figure 2. Statistics at $k\rho_p = 0.8$ for $\sim 2.6 \times 10^5$ time segments between 2005 and 2015: (a) distribution of $|\sigma_k|$, (b) median of spectral index α_k , (c) median of the angle θ_{LB} , (d) medians of α_k , where different color curves are for different ranges of solar wind speed V_p .

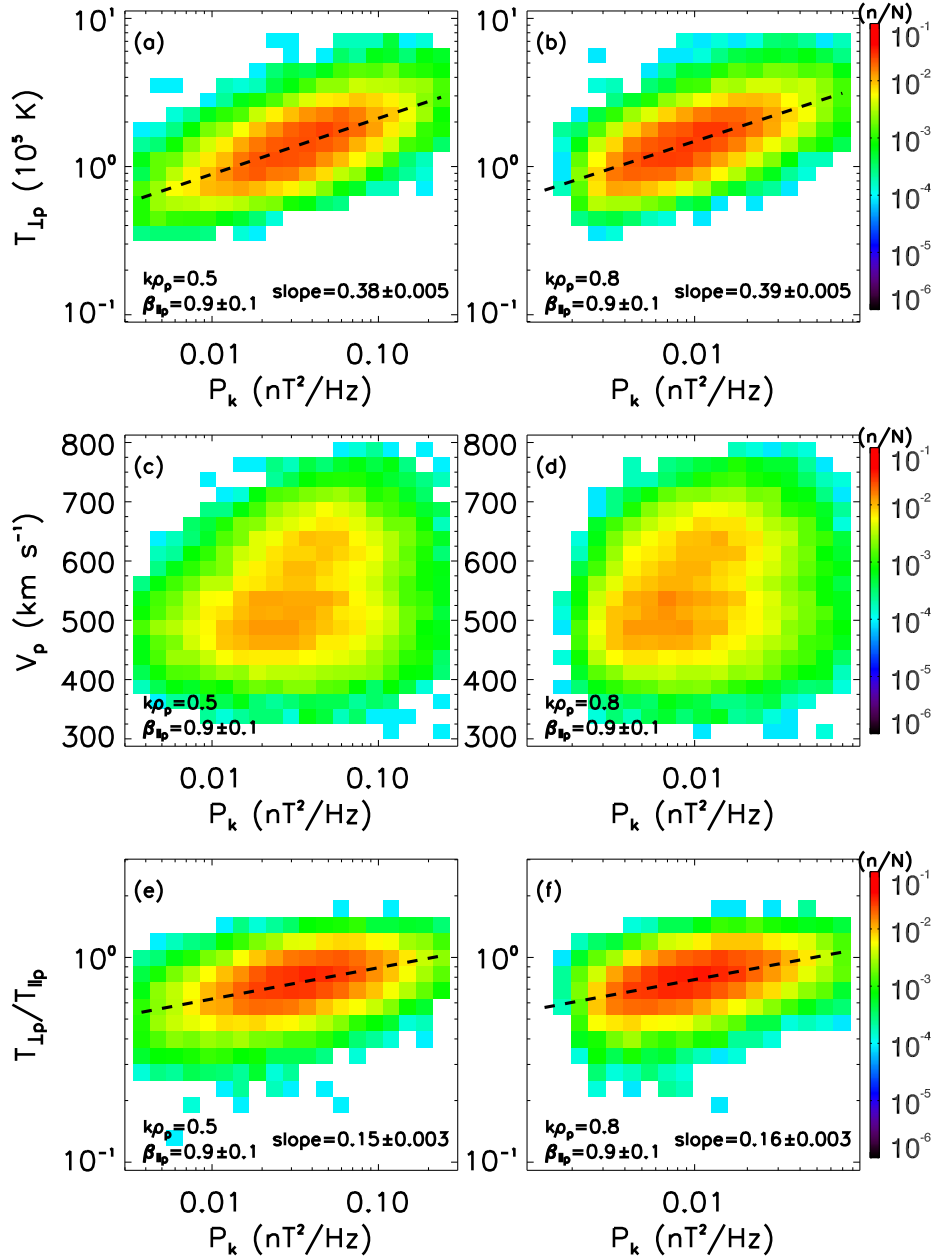


Figure 3. Top, middle, and bottom rows are distributions of $(P_k, T_{\perp p})$, (P_k, V_p) , and $(P_k, T_{\perp p}/T_{\parallel p})$, respectively. Left panels are for the wavenumber $k\rho_p = 0.5$ while right panels are for $k\rho_p = 0.8$. The black dashed lines are the linear fitting of the data in logarithmic space, and n and N represent the data number in each pixel and the total data number in each panel ($\sim 2.3 \times 10^4$), respectively.

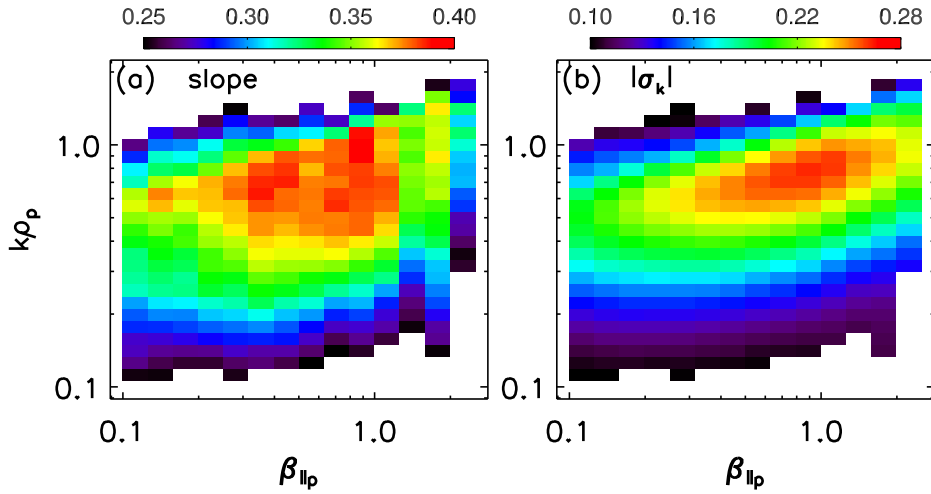


Figure 4. Color scale plot for (a) slopes of fitting lines of $(P_k, T_{\perp p})$ and (b) medians of $|\sigma_k|$ in the $(\beta_{\parallel p}, k)$ space.

correlation between $T_{\perp p}$ and P_k remains for each sub-dataset. The slopes of fitting lines decrease relative to those without the limitation of V_p , but are still considerable. We therefore believe that the correlation between $T_{\perp p}$ and P_k is inherent and can not be fully attributed to the scaling with the solar wind speed.

We have also investigated the possible correlation between the temperature ratio $T_{\perp p}/T_{\parallel p}$ and P_k , where $T_{\parallel p}$ is the proton parallel temperature. The temperature ratio is a critical parameter in the solar wind data analyses (Zhao, Feng, et al., 2019; Woodham et al., 2019), as well as in magnetosheath studies (Maruca et al., 2018). Figures 3e and 3f present the distributions of $(P_k, T_{\perp p}/T_{\parallel p})$ at scales of (e) $k\rho_p = 0.5$ and (f) $k\rho_p = 0.8$. One can find a trend that higher P_k corresponds to larger $T_{\perp p}/T_{\parallel p}$. This implies a correlation between $T_{\perp p}/T_{\parallel p}$ and P_k , whereas this correlation is weaker than that between $T_{\perp p}$ and P_k . The slopes of fitting lines of $(P_k, T_{\perp p}/T_{\parallel p})$ are around 0.15 in both cases. If we use different datasets by changing the range of $\beta_{\parallel p}$ and V_p , the correlation remains. The slopes of fitting lines may rise when $\beta_{\parallel p}$ decreases, but they are usually less than 0.25. A large $T_{\perp p}/T_{\parallel p}$ may excite proton cyclotron and mirror instabilities, which depends on the proton beta and plays a role in constraining the solar wind plasma (Hellinger et al., 2006).

It is notable that the correlation between $T_{\perp p}$ and P_k with considerable slopes exists in particular at proton scales; at larger scales the correlation weakens greatly. Figure 4a displays the slopes for cases with various k as well as $\beta_{\parallel p}$. In each case half of data with higher $|\sigma_k|$ are used to fit the data since higher $|\sigma_k|$ contributes to a better correlation. Any case with a slope < 0.25 or relative uncertainty greater than 10% is marked by the white color. One can see that a highlight region arises at scales $0.3 \lesssim k\rho_p \lesssim 1$ for finite $\beta_{\parallel p}$ ($\lesssim 2$), where the slopes are considerably large ($\gtrsim 0.35$). The slopes depend weakly on $\beta_{\parallel p}$ and have a peak value of 0.4 at $\beta_{\parallel p} \sim 0.9$. At smaller scales with $k\rho_p > 1$, the result is not clear because at these scales the instrument noise and/or aliasing may be non-negligible (Klein et al., 2014).

As somewhat expected, the large slopes in Figure 4a are accompanied by enhanced magnetic helicity. Using the same data in Figure 4a, Figure 4b plots medians of $|\sigma_k|$ and produces a comparable color region in the $(\beta_{\parallel p}, k)$ space. The comparability between Figures 4a and 4b confirms that higher $|\sigma_k|$ contributes to a better correlation between $T_{\perp p}$ and P_k . Further investigation on spectral index α_k (not shown) reveals that energy spectra in the highlight regions are steeper and have indices usually lower than $-7/3$,

which could be interpreted as hint of the occurrence of turbulent dissipation in the high-light regions. According to Figure 4, on the other hand, there appears an increasing trend of $k\rho_p$ with $\beta_{\parallel p}$ for a given slope or $|\sigma_k|$. Such a trend may be related to the increasing trend of $k_b\rho_p$ (dimensionless spectral break position) with $\beta_{\parallel p}$, as found by Duan et al. (2020).

4 Summary and Discussion

This letter performs a statistical research using in-situ measurements of the solar wind lasting for 11 years. For the nearly collisionless solar wind turbulence at proton scales, two new results are obtained as follows. Firstly, the turbulence with a higher magnetic helicity corresponds to a steeper energy spectrum statistically. Secondly, for the turbulence with high helicity ($|\sigma_k| > 0.15$), there exists a positive correlation between the proton perpendicular temperature and the turbulent magnetic energy at scales $0.3 \lesssim k\rho_p \lesssim 1$. The correlation can usually be described by a power law and its slope is considerable ($\gtrsim 0.35$) for $\beta_{\parallel p} \lesssim 2$. In addition, our examination on the nature of the solar wind turbulence supports the model of KAW turbulence at proton scales.

Based on our findings and existing literatures, we propose a scenario for solar wind turbulence and heating as follows. The magnetic fluctuations in the energy-containing range first undergo the Kolmogorov cascade in the inertial range, and predominantly become KAW turbulence at proton scales. The KAW turbulence raises magnetic helicity signature on the one hand, and suffers from dissipation on the other hand. Consequently, part of the magnetic energy goes into protons and a steeper energy spectrum with an index lower than $-7/3$ emerges. During this process, the fluctuations with higher initial energy in the energy-containing range, therefore higher energy at proton scales, will have greater ability to heat protons and result in higher proton temperatures. In other words, the higher temperatures are attributed to higher turbulent energy at proton scales that comes from stronger large-scale magnetic fluctuations by turbulent cascade.

As for the mechanisms of the heating, we propose cyclotron resonance and/or stochastic heating by the proton-scale KAW turbulence. Cyclotron resonance between KAWs and protons is possible, leading to the proton temperature increase in the direction perpendicular to the background magnetic field (Leamon et al., 1999; Gary & Borovsky, 2004; He, Wang, et al., 2015; Isenberg & Vasquez, 2019). The heating by turbulent KAWs can also be expected when stochastic heating arises due to the presence of large-amplitude electromagnetic fluctuations at the proton gyroscale (Johnson & Cheng, 2001; Chandran et al., 2010). Both mechanisms contribute to the perpendicular heating and are in agreement with our observations. These observations show that the power-law correlation related to the proton perpendicular temperature ($T_{\perp p}$) is the best correlation compared with the case for either the parallel temperature ($T_{\parallel p}$) or the total temperature (T_p). The correlation between T_p and P_k is secondary with a slope always < 0.35 , and becomes much weaker between $T_{\parallel p}$ and P_k . On the other hand, we remind that ion cyclotron waves (ICWs) in the solar wind may also contribute to the proton perpendicular heating. An analysis on the solar wind with time interval of 13.4 hours shows that the distribution of $(\beta_{\parallel p}, T_{\perp p}/T_{\parallel p})$ associated with ICWs corresponds to higher $T_{\perp p}/T_{\parallel p}$ (Telloni & Bruno, 2016). Direct measurements of the dissipation rate spectrum around ion scales in magnetosheath turbulence indicate the perpendicular heating by ICWs (He et al., 2019, 2020). In this letter, we favor the scenario of the heating by KAW turbulence because the KAW turbulence appears to be ubiquitous and has energy much higher than ICWs in the solar wind near 1 AU (He et al., 2012b). We note that the present scenario is preliminary and more investigations are required in future works.

Finally, we emphasize that the present research is relevant to the frequent observations of high ion perpendicular temperatures in the solar wind and potentially to those in the solar corona (Hollweg & Isenberg, 2002; Stansby et al., 2019). The data used in

this letter are from measurements near 1 AU. Other data, especially produced by the Solar Probe Plus spacecraft in the inner heliosphere (Fox et al., 2016), should be helpful for further studies.

Acknowledgments

The authors acknowledge the SWE team and MFI team on Wind for providing the data, which are publicly available via the Coordinated Data Analysis Web https://cdaweb.gsfc.nasa.gov/cdaweb/istp_public/. G.Q.Z. is grateful to the hospitality by Auburn University in USA as a visiting scholar. This research was supported by NSF under grant Nos. 41874204, 41974197, 41674170, 41531071, 11873018, 41804163, 11903016, and supported partly by scientific projects from Henan Province (19HASTIT020,16B140003). The authors acknowledge two referees for useful suggestions that improved this paper.

References

- Alexandrova, O., Chen, C. H. K., Sorriso-Valvo, L., Horbury, T. S., & Bale, S. D. (2013, October). Solar wind turbulence and the role of ion instabilities. *Space Sci. Rev.*, *178*(2-4), 101-139. doi: 10.1007/s11214-013-0004-8
- Bale, S. D., Kellogg, P. J., Mozer, F. S., Horbury, T. S., & Reme, H. (2005, June). Measurement of the electric fluctuation spectrum of magnetohydrodynamic turbulence. *Phys. Rev. Lett.*, *94*(21), 215002. doi: 10.1103/PhysRevLett.94.215002
- Bowen, T. A., Mallet, A., Huang, J., Klein, K. G., Malaspina, D. M., Stevens, M., ... Whittlesey, P. (2020, February). Ion-scale electromagnetic waves in the inner heliosphere. *The Astrophysical Journal Supplement Series*, *246*(2), 66. doi: 10.3847/1538-4365/ab6c65
- Bruno, R., & Carbone, V. (2013, May). The solar wind as a turbulence laboratory. *Living Reviews in Solar Physics*, *10*, 2. doi: 10.12942/lrsp-2013-2
- Bruno, R., Trenchi, L., & Telloni, D. (2014, September). Spectral slope variation at proton scales from fast to slow solar wind. *The Astrophysical Journal Letters*, *793*(1), L15. doi: 10.1088/2041-8205/793/1/L15
- Chandran, B. D. G., Li, B., Rogers, B. N., Quataert, E., & Germaschewski, K. (2010, September). Perpendicular ion heating by low-frequency Alfvén-wave turbulence in the solar wind. *The Astrophysical Journal*, *720*, 503-515. doi: 10.1088/0004-637X/720/1/503
- Duan, D., Bowen, T. A., Chen, C. H. K., Mallet, A., He, J., Bale, S. D., ... Whittlesey, P. (2020, February). The radial dependence of proton-scale magnetic spectral break in slow solar wind during PSP Encounter 2. *The Astrophysical Journal Supplement Series*, *246*(2), 55. doi: 10.3847/1538-4365/ab672d
- Fox, N. J., Velli, M. C., Bale, S. D., Decker, R., Driesman, A., Howard, R. A., ... Szabo, A. (2016, December). The solar probe plus mission: humanity's first visit to our star. *Space Sci. Rev.*, *204*(1-4), 7-48. doi: 10.1007/s11214-015-0211-6
- Galtier, S. (2006, January). Wave turbulence in incompressible Hall magnetohydrodynamics. *Journal of Plasma Physics*, *72*(5), 721-769. doi: 10.1017/S0022377806004521
- Gary, S. P., & Borovsky, J. E. (2004, June). Alfvén-cyclotron fluctuations: Linear Vlasov theory. *Journal of Geophysical Research (Space Physics)*, *109*(A6), A06105. doi: 10.1029/2004JA010399
- Gary, S. P., & Smith, C. W. (2009, December). Short-wavelength turbulence in the solar wind: Linear theory of whistler and kinetic Alfvén fluctuations. *Journal of Geophysical Research (Space Physics)*, *114*(A12), A12105. doi: 10.1029/2009JA014525
- Gary, S. P., Yin, L., & Winske, D. (2006, June). Alfvén-cyclotron scattering of

- solar wind ions: Hybrid simulations. *Journal of Geophysical Research (Space Physics)*, *111*, A06105. doi: 10.1029/2005JA011552
- Grošelj, D., Mallet, A., Loureiro, N. F., & Jenko, F. (2018, March). Fully kinetic simulation of 3D kinetic Alfvén turbulence. *Phys. Rev. Lett.*, *120*(10), 105101. doi: 10.1103/PhysRevLett.120.105101
- He, J., Duan, D., Wang, T., Zhu, X., Li, W., Verscharen, D., . . . Burch, J. (2019, August). Direct measurement of the dissipation rate spectrum around ion kinetic scales in space plasma turbulence. *The Astrophysical Journal*, *880*(2), 121. doi: 10.3847/1538-4357/ab2a79
- He, J., Marsch, E., Tu, C., Yao, S., & Tian, H. (2011, April). Possible evidence of Alfvén-cyclotron waves in the angle distribution of magnetic helicity of solar wind turbulence. *The Astrophysical Journal*, *731*, 85. doi: 10.1088/0004-637X/731/2/85
- He, J., Pei, Z., Wang, L., Tu, C., Marsch, E., Zhang, L., & Salem, C. (2015, June). Sunward propagating Alfvén waves in association with sunward drifting proton beams in the solar wind. *The Astrophysical Journal*, *805*, 176. doi: 10.1088/0004-637X/805/2/176
- He, J., Tu, C., Marsch, E., & Yao, S. (2012a, January). Do oblique Alfvén/ion-cyclotron or fast-mode/whistler waves dominate the dissipation of solar wind turbulence near the proton inertial length? *The Astrophysical Journal Letters*, *745*, L8. doi: 10.1088/2041-8205/745/1/L8
- He, J., Tu, C., Marsch, E., & Yao, S. (2012b, April). Reproduction of the observed two-component magnetic helicity in solar wind turbulence by a superposition of parallel and oblique Alfvén waves. *The Astrophysical Journal*, *749*, 86. doi: 10.1088/0004-637X/749/1/86
- He, J., Wang, L., Tu, C., Marsch, E., & Zong, Q. (2015, February). Evidence of Landau and cyclotron resonance between protons and kinetic waves in solar wind turbulence. *The Astrophysical Journal Letters*, *800*(2), L31. doi: 10.1088/2041-8205/800/2/L31
- He, J., Zhu, X., Verscharen, D., Duan, D., Zhao, J., & Wang, T. (2020, July). Spectra of diffusion, dispersion, and dissipation for kinetic Alfvénic and compressive turbulence: comparison between kinetic theory and measurements from MMS. *The Astrophysical Journal*, *898*(1), 43. doi: 10.3847/1538-4357/ab9174
- Hellinger, P., Trávníček, P., Kasper, J. C., & Lazarus, A. J. (2006, May). Solar wind proton temperature anisotropy: linear theory and WIND/SWE observations. *Geophysical Research Letters*, *33*, L09101. doi: 10.1029/2006GL025925
- Hollweg, J. V., & Isenberg, P. A. (2002, July). Generation of the fast solar wind: a review with emphasis on the resonant cyclotron interaction. *Journal of Geophysical Research (Space Physics)*, *107*, 1147. doi: 10.1029/2001JA000270
- Howes, G. G., Dorland, W., Cowley, S. C., Hammett, G. W., Quataert, E., Schekochihin, A. A., & Tatsuno, T. (2008, February). Kinetic simulations of magnetized turbulence in astrophysical plasmas. *Phys. Rev. Lett.*, *100*(6), 065004. doi: 10.1103/PhysRevLett.100.065004
- Howes, G. G., McCubbin, A. J., & Klein, K. G. (2018, February). Spatially localized particle energization by Landau damping in current sheets produced by strong Alfvén wave collisions. *Journal of Plasma Physics*, *84*(1), 905840105. doi: 10.1017/S0022377818000053
- Howes, G. G., & Quataert, E. (2010, January). On the interpretation of magnetic helicity signatures in the dissipation range Of solar wind turbulence. *The Astrophysical Journal Letters*, *709*(1), L49-L52. doi: 10.1088/2041-8205/709/1/L49
- Isenberg, P. A., & Vasquez, B. J. (2019, December). Perpendicular ion heating by cyclotron resonant dissipation of turbulently generated kinetic Alfvén waves in the solar wind. *The Astrophysical Journal*, *887*(1), 63. doi: 10.3847/1538-4357/ab4e12

- Johnson, J. R., & Cheng, C. Z. (2001). Stochastic ion heating at the magnetopause due to kinetic Alfvén waves. *Geophysical Research Letters*, *28*, 4421-4424. doi: 10.1029/2001GL013509
- Kasper, J. C., Lazarus, A. J., & Gary, S. P. (2008, December). Hot solar-wind helium: direct evidence for local heating by Alfvén-cyclotron dissipation. *Phys. Rev. Lett.*, *101*(26), 261103. doi: 10.1103/PhysRevLett.101.261103
- Kasper, J. C., Lazarus, A. J., Steinberg, J. T., Ogilvie, K. W., & Szabo, A. (2006, March). Physics-based tests to identify the accuracy of solar wind ion measurements: a case study with the Wind Faraday Cups. *Journal of Geophysical Research (Space Physics)*, *111*, A03105. doi: 10.1029/2005JA011442
- Kasper, J. C., Maruca, B. A., Stevens, M. L., & Zaslavsky, A. (2013, March). Sensitive test for ion-cyclotron resonant heating in the solar wind. *Phys. Rev. Lett.*, *110*(9), 091102. doi: 10.1103/PhysRevLett.110.091102
- Klein, K. G., Howes, G. G., TenBarge, J. M., & Podesta, J. J. (2014, April). Physical interpretation of the angle-dependent magnetic helicity spectrum in the solar wind: the nature of turbulent fluctuations near the proton gyroradius scale. *The Astrophysical Journal*, *785*(2), 138. doi: 10.1088/0004-637X/785/2/138
- Leamon, R. J., Smith, C. W., Ness, N. F., & Wong, H. K. (1999, October). Dissipation range dynamics: kinetic Alfvén waves and the importance of β_e . *Journal of Geophysical Research*, *104*(A10), 22331-22344. doi: 10.1029/1999JA900158
- Lepping, R. P., Acuña, M. H., Burlaga, L. F., Farrell, W. M., Slavin, J. A., Schatten, K. H., ... Worley, E. M. (1995, February). The wind magnetic field investigation. *Space Sci. Rev.*, *71*, 207-229. doi: 10.1007/BF00751330
- Livi, S., Marsch, E., & Rosenbauer, H. (1986, July). Coulomb collisional domains in the solar wind. *Journal of Geophysical Research*, *91*, 8045-8050. doi: 10.1029/JA091iA07p08045
- Markovskii, S. A., & Vasquez, B. J. (2013, May). Magnetic helicity in the dissipation range of strong imbalanced turbulence. *The Astrophysical Journal*, *768*(1), 62. doi: 10.1088/0004-637X/768/1/62
- Marsch, E., Schwenn, R., Rosenbauer, H., Muehlhaeuser, K.-H., Pilipp, W., & Neubauer, F. M. (1982, January). Solar wind protons - three-dimensional velocity distributions and derived plasma parameters measured between 0.3 and 1 AU. *Journal of Geophysical Research*, *87*, 52-72. doi: 10.1029/JA087iA01p00052
- Maruca, B. A., Chasapis, A., Gary, S. P., Band yopadhyay, R., Chhiber, R., Parashar, T. N., ... Strangeway, R. J. (2018, October). MMS observations of beta-dependent constraints on ion temperature anisotropy in Earth's magnetosheath. *The Astrophysical Journal*, *866*(1), 25. doi: 10.3847/1538-4357/aaddfb
- Matthaeus, W. H., & Goldstein, M. L. (1982, August). Measurement of the rugged invariants of magnetohydrodynamic turbulence in the solar wind. *Journal of Geophysical Research*, *87*, 6011-6028. doi: 10.1029/JA087iA08p06011
- Newbury, J. A., Russell, C. T., Phillips, J. L., & Gary, S. P. (1998, May). Electron temperature in the ambient solar wind: typical properties and a lower bound at 1 AU. *Journal of Geophysical Research*, *103*(A5), 9553-9566. doi: 10.1029/98JA00067
- Ogilvie, K. W., Chornay, D. J., Fritzenreiter, R. J., Hunsaker, F., Keller, J., Lobell, J., ... Gergin, E. (1995, February). SWE, a comprehensive plasma instrument for the wind spacecraft. *Space Sci. Rev.*, *71*, 55-77. doi: 10.1007/BF00751326
- Osman, K. T., Matthaeus, W. H., Greco, A., & Servidio, S. (2011, January). Evidence for inhomogeneous heating in the solar wind. *The Astrophysical Journal Letters*, *727*(1), L11. doi: 10.1088/2041-8205/727/1/L11
- Osman, K. T., Matthaeus, W. H., Wan, M., & Rappazzo, A. F. (2012, June). Intermittency and local heating in the solar wind. *Phys. Rev. Lett.*, *108*(26), 261102. doi: 10.1103/PhysRevLett.108.261102

- Parashar, T. N., Salem, C., Wicks, R. T., Karimabadi, H., Gary, S. P., & Matthaeus, W. H. (2015, October). Turbulent dissipation challenge: a community-driven effort. *Journal of Plasma Physics*, *81*(5), 905810513. doi: 10.1017/S0022377815000860
- Perri, S., Goldstein, M. L., Dorelli, J. C., & Sahraoui, F. (2012, November). Detection of small-scale structures in the dissipation regime of solar-wind turbulence. *Phys. Rev. Lett.*, *109*(19), 191101. doi: 10.1103/PhysRevLett.109.191101
- Podesta, J. J. (2013, September). Evidence of kinetic Alfvén waves in the solar wind at 1 AU. *Sol. Phys.*, *286*(2), 529-548. doi: 10.1007/s11207-013-0258-z
- Sahraoui, F., Goldstein, M. L., Robert, P., & Khotyaintsev, Y. V. (2009, June). Evidence of a cascade and dissipation of solar-wind turbulence at the electron gyroscale. *Phys. Rev. Lett.*, *102*(23), 231102. doi: 10.1103/PhysRevLett.102.231102
- Sahraoui, F., Huang, S. Y., Belmont, G., Goldstein, M. L., Réтино, A., Robert, P., & De Patoul, J. (2013, November). Scaling of the electron dissipation range of Solar Wind turbulence. *The Astrophysical Journal*, *777*(1), 15. doi: 10.1088/0004-637X/777/1/15
- Schwenn, R. (2006, June). Solar wind sources and their variations over the solar cycle. *Space Sci. Rev.*, *124*, 51-76. doi: 10.1007/s11214-006-9099-5
- Smith, C. W., Vasquez, B. J., & Hollweg, J. V. (2012, January). Observational constraints on the role of cyclotron damping and kinetic Alfvén waves in the solar wind. *The Astrophysical Journal*, *745*(1), 8. doi: 10.1088/0004-637X/745/1/8
- Sonnerup, B. U. Ö., & Scheible, M. (1998). Minimum and maximum variance analysis. *ISSI Scientific Reports Series*, *1*, 185-220.
- Stansby, D., Perrone, D., Matteini, L., Horbury, T. S., & Salem, C. S. (2019, March). Alpha particle thermodynamics in the inner heliosphere fast solar wind. *Astronomy and Astrophysics*, *623*, L2. doi: 10.1051/0004-6361/201834900
- Taylor, G. I. (1938, February). The Spectrum of Turbulence. *Proceedings of the Royal Society of London Series A*, *164*(919), 476-490. doi: 10.1098/rspa.1938.0032
- Telloni, D., & Bruno, R. (2016, November). Linking fluid and kinetic scales in solar wind turbulence. *Mon. Not. R. Astron. Soc.*, *463*(1), L79-L83. doi: 10.1093/mnrasl/slw135
- Tu, C.-Y., & Marsch, E. (1995, July). MHD structures, waves and turbulence in the solar wind: Observations and theories. *Space Sci. Rev.*, *73*, 1-210. doi: 10.1007/BF00748891
- Verscharen, D., Klein, K. G., & Maruca, B. A. (2019, December). The multi-scale nature of the solar wind. *Living Reviews in Solar Physics*, *16*(1), 5. doi: 10.1007/s41116-019-0021-0
- Wang, T., Alexandrova, O., Perrone, D., Dunlop, M., Dong, X., Bingham, R., . . . Burch, J. L. (2019, February). Magnetospheric multiscale observation of kinetic signatures in the Alfvén vortex. *The Astrophysical Journal Letters*, *871*, L22. doi: 10.3847/2041-8213/aafe0d
- Woodham, L. D., Wicks, R. T., Verscharen, D., Owen, C. J., Maruca, B. A., & Alterman, B. L. (2019, October). Parallel-propagating fluctuations at proton-kinetic scales in the solar wind are dominated by kinetic instabilities. *The Astrophysical Journal Letters*, *884*(2), L53. doi: 10.3847/2041-8213/ab4adc
- Wu, D. J., & Chen, L. (2020). *Kinetic Alfvén waves in laboratory, space, and astrophysical plasmas*. Singapore: Springer. doi: 10.1007/978-981-13-7989-5
- Zhao, G. Q., Feng, H. Q., Wu, D. J., Huang, J., Zhao, Y., Liu, Q., & Tian, Z. J. (2020, January). Dependence of ion temperatures on alpha-proton differential flow vector and heating mechanisms in the solar wind. *The Astrophysical Journal Letters*, *889*(1), L14. doi: 10.3847/2041-8213/ab6b29

- Zhao, G. Q., Feng, H. Q., Wu, D. J., Liu, Q., Zhao, Y., Zhao, A., & Huang, J. (2018, March). Statistical study of low-frequency electromagnetic cyclotron waves in the solar wind at 1 AU. *Journal of Geophysical Research (Space Physics)*, *123*, 1715-1730. doi: 10.1002/2017JA024979
- Zhao, G. Q., Feng, H. Q., Wu, D. J., Pi, G., & Huang, J. (2019, February). On the generation mechanism of electromagnetic cyclotron waves in the solar wind: statistical results from Wind observations. *The Astrophysical Journal*, *871*, 175. doi: 10.3847/1538-4357/aaf8b8
- Zhao, G. Q., Li, H., Feng, H. Q., Wu, D. J., Li, H. B., & Zhao, A. (2019, October). Effects of alpha-proton differential flow on proton temperature anisotropy instabilities in the solar wind: Wind observations. *The Astrophysical Journal*, *884*(1), 60. doi: 10.3847/1538-4357/ab3d35